ACS APPLIED MATERIALS & INTERFACES

Research Article

www.acsami.org

# Recovery of Nonwetting Characteristics by Surface Modification of Gallium-Based Liquid Metal Droplets Using Hydrochloric Acid Vapor

Daeyoung Kim,[†] Peter Thissen,[‡] Gloria Viner,[§] Dong-Weon Lee,[▽] Wonjae Choi,[§] Yves J. Chabal,[‡] and Jeong-Bong (J.B.) Lee*,[†]

[†]Department of Electrical Engineering, The University of Texas at Dallas, 800 West Campbell Rd., Richardson, Texas 75080, United States

[‡]Department of Materials Science and Engineering, The University of Texas at Dallas, 800 West Campbell Rd., Richardson, Texas 75080, United States

[§]Department of Mechanical Engineering, The University of Texas at Dallas, 800 West Campbell Rd., Richardson, Texas 75080, United States

[▽]School of Mechanical Systems Engineering, Chonnam National University, 77 Yongbong-ro, Buk-Gu, Gwangju, 550-757, South Korea

**ABSTRACT:** The applicability of gallium-based liquid metal alloy has been limited by the oxidation problem. In this paper, we report a simple method to remove the oxide layer on the surface of such alloy to recover its nonwetting characteristics, using hydrochloric acid (HCl) vapor. Through the HCl vapor treatment, we successfully restored the nonwetting characteristics of the alloy and suppressed its viscoelasticity. We analyzed the change of surface chemistry before and after the HCl vapor treatment using X-ray photoelectron spectroscopy (XPS) and low-energy ion-scattering spectroscopy (LEIS). Results showed that the oxidized surface of the commercial gallium-based alloy Galinstan ($Ga_2O_3$ and $Ga_2O$) was replaced with $InCl_3$ and $GaCl_3$ after the treatment. Surface tension and static contact angle on a Teflon-coated glass of the HCl-vapor-treated Galinstan were measured to be 523.8 mN/m and 152.5°. A droplet bouncing test was successfully carried out to demonstrate the nonwetting characteristics of the HCl-vapor-treated Galinstan. Finally, the stability of the transformed surface of the HCl-vapor-treated Galinstan was investigated by measuring the contact angle and LEIS spectra after reoxidation in an ambient environment.

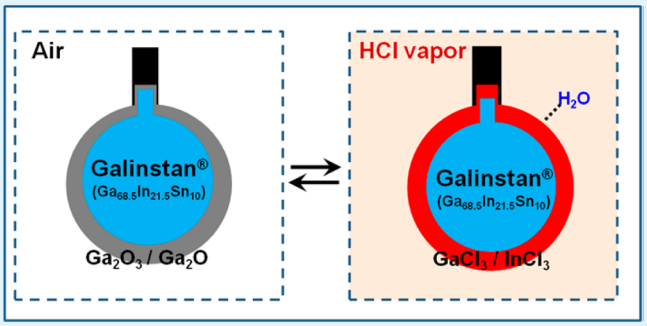


**KEYWORDS:** *HCl vapor treatment, surface modification, gallium-based liquid metal alloy, nonwetting, Galinstan*

## INTRODUCTION

Liquid metal, i.e., a metal that is in liquid phase at or near room temperature, has a wide range of applications, because of its high thermal and electrical conductivity, combined with its infinite deformability. Mercury is one of the most well-known liquid metals, but its toxicity poses a threat to human health and environment. Recently, gallium-based eutectic alloy has emerged as a potential alternative to mercury, because its toxicity is negligible[1] and its melting point is sufficiently low (−19 °C for Galinstan, which is a commercially available gallium-based alloy). Gallium-based binary (e.g., EGaIn[2]) and ternary alloys (e.g., Galinstan) were investigated for various applications including microcooling,[3] electrical interconnection,[4] microsyringe for cells,[5] radio-frequency switch,[6] magneto-hydrodynamic pump,[7] stretchable antenna,[8] and tunable-frequency selective surface.[9]

Although a gallium-based alloy has a great potential for a variety of promising applications, the surface of gallium-based alloy instantly oxidizes in ambient environment and turns into a thin layer of gallium oxide ($Ga_2O_3$ and $Ga_2O$).[10] This oxide layer is solid and remains elastic unless it experiences a yield stress; thus, the oxidized gallium-based alloy does not behave like a simple liquid. Moreover, the oxide layer of gallium-based alloy is known to adhere to almost any solid surface, causing a severe stiction problem.[10] There have been a few studies to overcome such unfavorable characteristics of gallium-based liquid metal. Liu et al. found that Galinstan does not oxidize when the concentration of oxygen is below 1 ppm.[11] Maintaining such an environment, however, requires a very tight and costly hermetic packaging. Zrnick and Swatik found that it is possible to remove the oxide layer by treating the surface with diluted HCl solution,[12] and Dickey et al. applied the technique for microfluidic applications to observe the alloy does not suffer from viscoelasticity or wetting.[2] Although the

Received: October 16, 2012
Accepted: December 3, 2012
Published: December 3, 2012

  

HCl solution-based method to remove the oxidized surface of gallium-based liquid metal (even mercury[13]) is very reliable, the practical applicability of the approach is limited as the liquid metal needs to be immersed in the solution.

In this paper, we report a method based on HCl vapor to modify the surface of the oxidized gallium-based alloy from $Ga_2O_3/Ga_2O$ to $GaCl_3/InCl_3$, resulting in the recovery of nonwetting characteristics of Galinstan droplet. Analysis of the surface chemistry of Galinstan droplet using XPS and LEIS before and after the HCl vapor treatment, along with contact angles and surface tension measurements, are reported. The stability of the modified surface is also investigated by exposing the HCl-vapor-treated Galinstan to the atmosphere and tracking the change of contact angles and LEIS spectra.

## EXPERIMENTAL SECTION

**Materials.** Galinstan was purchased from Geratherm Medical AG and used as-received. The composition rate of Galinstan is 68.5% gallium, 21.5% indium, and 10% tin.

**Static Contact Angle Measurements.** We used three types of glass slides: a bare soda–lime glass slide (Corning Life Science); a Cytop-coated glass (spin-coated with CTX-809A from Asahi Glass Co. and cured at 185 °C; thickness of cured Cytop layer ≈ 1 μm); and a Teflon-coated glass (spin-coated with 6% Teflon AF solution from DuPont and cured at 165 °C; thickness of cured Teflon layer ≈ 30 nm). On these substrates, we deposited ∼8 μL Galinstan droplets, using a pipet, and we measured the static contact angles using a goniometer (Ramé-Hart 260-F4). In this measurement, the static contact angles can reliably represent the wetting property of the Galinstan droplet before and after HCl vapor treatment, because the contact angle hysteresis on smooth surfaces was low. The condition for measuring the static contact angle was a humidity of 46.9 ± 0.8% and a temperature of 22.9 ± 0.2 °C.

**Surface Tension Measurements.** We used pendant drop method[14,15] to measure the surface tension of Galinstan before and after the HCl vapor treatment. A Ramé-Hart Model 260-F4 goniometer was used for the measurement, and the alloy was infused through a Teflon tip (inner diameter of 0.3 mm) to minimize the wetting. The ambient humidity and temperature were 46.9 ± 0.8% and 22.9 ± 0.2 °C, respectively.

**X-ray Photoelectron Spectroscopy (XPS).** XPS survey spectra were obtained for the oxidized Galinstan before and after the HCl vapor treatment. We used the PHI 5800 ESCA XPS system (Physical Electronics, Inc.) equipped with a concentric hemispherical analyzer. We used a monochromated aluminum X-ray radiation (1486.6 eV) with a spot diameter of 100 μm at a filament current of ∼23 mA. A ∼1.5 μL droplet of naturally oxidized Galinstan was deposited on a 1 cm × 2 cm silicon wafer. The sample was scanned under ultrahigh vacuum (UHV) ($10^{-9}$–$10^{-8}$ mTorr) conditions. The scanning was performed over a 100 μm × 100 μm area with a pass energy of 46.95 eV for survey and 11.75 eV for detailed scans. The takeoff angle of the reflected photoelectrons was 45°, with respect to the surface. All spectra were calibrated using the C 1s peak (binding energy of 285 eV) as an internal reference. CASA XPS software was used to analyze the obtained spectra, and MultiPak v9 software was used to measure the surface sensitivity factors and the atomic concentration.

**Low-Energy Ion Scattering Spectroscopy (LEIS).** We also performed low-energy ion scattering spectroscopy (LEIS) analysis on a Galinstan droplet before and after HCl vapor treatment. Qtac analyzer (ION-TOF GmbH, Münster, Germany) was used to apply a 3.0 keV $^4He^+$ beam, with a current of 2.3 nA and a fixed scatter angle of 145°. Each measurement lasted for 120 s. The fraction of backscattered He ions was measured as a function of the kinetic energy with a double toroidal analyzer, imaging the ions according to their energy onto a position-sensitive electrostatic detector. It is essential to use the combination of analyzer-detector settings; the large scatter angle of detection, combined with the parallel detection, increases the sensitivity by orders of magnitude, and allows the overall ion dose needed for measurement to be reduced.[16] As such, the total ion dose is very low, compared to the surface atomic density; therefore, ion-induced sputtering and intermixing are negligible.

## RESULTS AND DISCUSSION

**Physical Properties.** Figures 1a, 1c, and 1e show the droplets of naturally oxidized Galinstan on three types of substrates (bare glass, Cytop-coated glass, and Teflon-coated glass, respectively) before the HCl vapor treatment. Viscoelasticity that was due to the presence of the oxide ($Ga_2O_3/Ga_2O$) layer caused the shape of the droplets to be asymmetric and irregular. The contact angle of a liquid droplet on a flat solid surface is determined using Young's equation:[17]

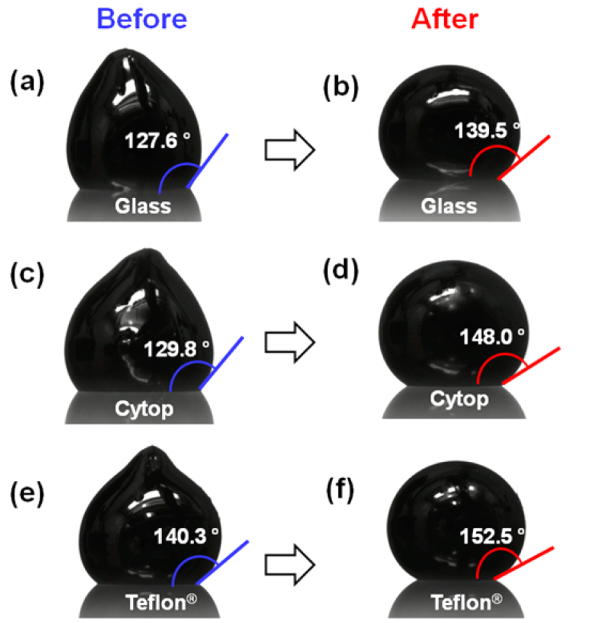


**Figure 1.** Contact angle of Galinstan droplets on (a, b) a bare glass slide, (c, d) Cytop-coated glass slide, and (e, f) Teflon-coated glass slide, before (panels a, c, and e) and after (panels b, d, and f) the HCl vapor treatment.

$$\cos\theta = \frac{\gamma_{SG} - \gamma_{SL}}{\gamma_{LG}} \quad (1)$$

where $\theta$ is the contact angle and $\gamma_{SG}$, $\gamma_{SL}$, and $\gamma_{LG}$ represent the surface tension of solid–gas, solid–liquid, and liquid–gas interfaces, respectively. Equation 1 predicts that the contact angle of a given liquid increases as the surface tension of the solid/gas interface decreases. The contact angle of the naturally oxidized Galinstan droplet on bare glass ($\gamma_{SG}$ ≈ 49.8 mN/m; Figure 1a)[18] was 127.6°. Higher contact angles ($\theta$ = 129.8° and 140.3°) were observed on glass slides coated with Cytop ($\gamma_{SG}$ ≈ 19.0 mN/m) and Teflon ($\gamma_{SG}$ ≈ 18.5 mN/m), as the surface


dx.doi.org/10.1021/am302357t | ACS Appl. Mater. Interfaces 2013, 5, 179–185

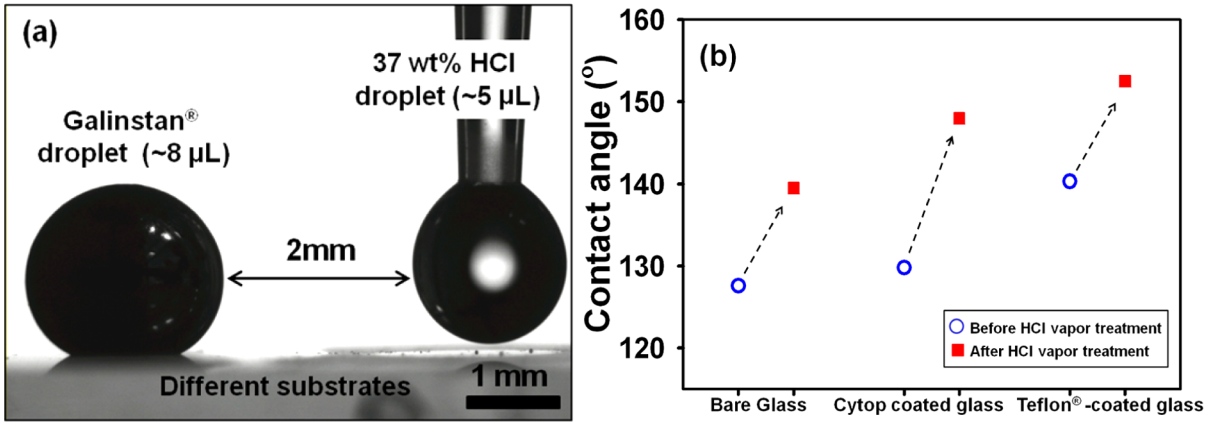


**Figure 2.** (a) Optical image of HCl vapor treatment of Galinstan droplet on different substrates. (b) Contact angles of Galinstan droplets on various substrates, before and after the HCl vapor treatment. The volume of the droplets was ~8 $\mu$L.

tension of these fluorocarbon polymers are much lower than that of the glass.[18,19]

In order to modify the surface of a naturally oxidized Galinstan droplet, we placed a pendant droplet of HCl (37 wt %, ~5 $\mu$L) 2 mm away from the Galinstan droplet (Figure 2a) for 15 s. HCl vapor evaporated and chemically reacted with the oxidized surface layer of the Galinstan droplet, causing a rapid change of contact angle of the Galinstan droplet. Figure 2b shows the contact angle changes of Galinstan droplet on three different substrates before and after the HCl vapor treatment. Figure 1b, 1d, and 1f show the Galinstan droplet images after the HCl vapor treatment.

We also directly measured the surface tension of Galinstan droplet before and after the HCl vapor treatment. Since the naturally oxidized Galinstan before the HCl vapor treatment is viscoelastic, its deformation is highly hysteretic and the measurement of its surface tension is prone to error. Figures 3a and 3c show two droplets of oxidized Galinstan with

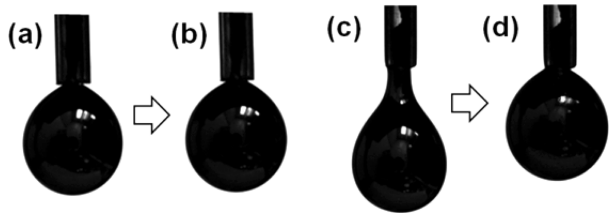


**Figure 3.** Pendant drop images of Galinstan droplets (a, c) before and (b, d) after HCl vapor treatment.

essentially identical volume, but showing drastically different shapes that are due to the viscoelasticity of the droplet. Therefore, surface tensions of these two droplets of the same liquid, measured by pendant drop method, were vastly different (420.3 and 217.3 mN/m, respectively). After the HCl vapor treatment, measured surface tensions of the Galinstan droplet were consistently 523.8 ± 25.4 mN/m (see Figures 3b and 3d). The measured surface tension is comparable to that of pure Galinstan (534.6 ± 10.7 mN/m), although the surface chemistry is not exactly the same.[11]

**Surface Chemistry.** The change of contact angles and surface tension clearly indicated that there was significant modification of surface chemistry of the Galinstan droplet before and after the HCl vapor treatment. We used XPS and LEIS to directly investigate how the surface chemistry changed with the HCl vapor treatment. Figure 4 shows XPS survey spectra for the naturally oxidized Galinstan before (Figure 4a)

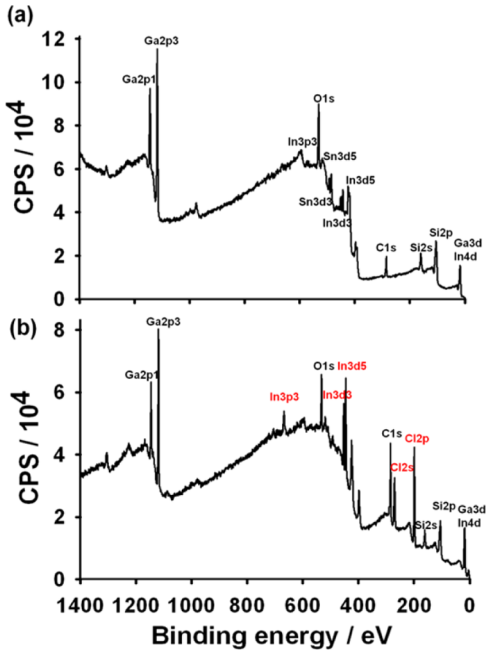


**Figure 4.** XPS survey spectra of Galinstan droplet on silicon substrate (a) before and (b) after HCl vapor treatment. (We believe that C 1s and unidentified peaks were from impurities.)

and after (Figure 4b) the treatment. As expected, the survey spectrum for the oxidized Galinstan shows gallium peaks from different orbitals such as Ga 2p and Ga 3d, weak indium peaks (In 3p, In 3d, and In 4d) as well as a tin peak (Sn 3d). In addition, Si 2s and Si 2p peaks and O 1s peaks were observed due to silicon substrate. The survey spectrum of the HCl-vapor-treated Galinstan also shows gallium, indium, and tin peaks. However, there was a clear difference between the two survey spectra as the second spectrum (from the HCl-vapor-treated Galinstan) shows strong indium peaks (In 3p and In 3d) and chlorine peaks (Cl 2s and Cl 2p).

Figure 5 shows high-resolution XPS spectra near O 1s, Ga 2p, Cl 2p, and In 3d orbitals. As shown in Figure 5a, before the HCl vapor treatment, two different oxide peaks for O 1s were observed; these peaks correspond to $SiO_2$ (binding energy =


dx.doi.org/10.1021/am302357t | ACS Appl. Mater. Interfaces 2013, 5, 179−185

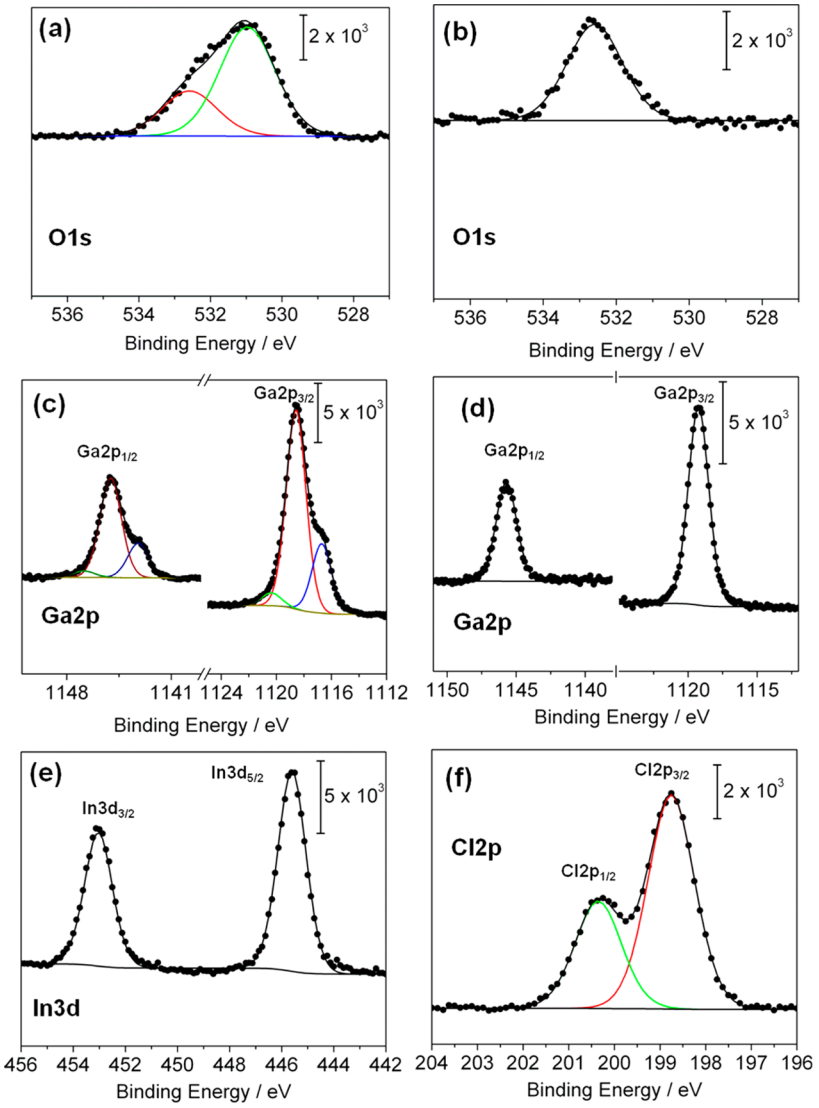


**Figure 5.** O 1s fitted XPS spectra of (a) the natively oxidized Galinstan and (b) the HCl-vapor-treated Galinstan. Ga 2p fitted XPS spectra of (c) the natively oxidized Galinstan and (d) the HCl-vapor-treated Galinstan. (e) In 3d fitted XPS spectra for the HCl-vapor-treated Galinstan. (f) Cl 2p fitted XPS spectra for the HCl-vapor-treated Galinstan.

532.5 eV)[20] and $Ga_2O_3$ (binding energy = 530.8 eV).[21] One can infer that the $SiO_2$ peak was from the native oxide on the surface of silicon substrate and $Ga_2O_3$ peak was from the oxidized surface of the Galinstan droplet.[10] Interestingly, the O 1s peak at 530.8 eV ($Ga_2O_3$ peak) completely vanished in the XPS spectrum after the HCl vapor treatment, as shown in Figure 5b. We speculated that $Ga_2O_3$ chemically reacted with HCl vapor and turned into gallium chloride ($GaCl_3$). This speculation was confirmed with fitted Ga 2p spectra obtained before (Figure 5c) and after the treatment (Figure 5d). Before the treatment, the photoelectron peak of Ga $2p_{3/2}$ was centered at a binding energy of 1120.4 ± 0.1 eV, corresponding to the $Ga^{3+}$ state. Combined with the O 1s peak at 530.8 eV, this observation suggests the existence of $Ga_2O_3$, although the binding energy is ∼1.5 eV higher than that in ref 10. The observed discrepancy might have occurred due to the presence of gallium suboxide state ($Ga_2O$, $Ga^+$ state), whose peak is located at 1118.5 ± 0.1 eV; this peak was absent in the previous reports.[10,22] In addition, the peak located at 1116.7 ± 0.1 eV corresponds to the metallic state of gallium.[10] After the treatment, only a single peak corresponding to $Ga^{3+}$ (binding energy = 1119.2 ± 0.1 eV)[23] was observed, which, in conjunction with the disappearance of the O 1s peak and the emergence of the Cl 2p peak after the treatment, indicates the appearance of $GaCl_3$, as a result of chemical reaction between gallium oxide ($Ga_2O_3$ and $Ga_2O$) and HCl vapor.

Figures 5e and 5f show the fitted In 3d and Cl 2p spectra after HCl vapor treatment; the In $3d_{3/2}$, In $3d_{5/2}$, and Cl $2p_{1/2}$, Cl $2p_{3/2}$ spin−orbital splitting photoelectrons were centered at binding energies of 453.1 ± 0.1 eV, 445.6 ± 0.1 eV, 200.2 ± 0.1 eV, and 198.7 ± 0.1 eV, respectively. Based on these spectra, we hypothesized that indium chloride ($InCl_3$) also formed on the surface of the Galinstan after HCl vapor treatment.[24] Based on the XPS study, we concluded that (i) the gallium oxide ($Ga_2O_3$ and $Ga_2O$) on the surface of the oxidized Galinstan changed to gallium chloride ($GaCl_3$), and (ii) HCl also reacted with indium beneath the surface layer to form indium chloride ($InCl_3$). As a result, the absence of oxide layer caused Galinstan to behave as a nonwetting, Newtonian liquid.

Although XPS is an excellent technique to analyze surface chemistry, the photoemitted electrons detected by the XPS technique are from 1−10 nm depth of the surface. In order to

further analyze surface chemistry of the Galinstan droplet on the outermost atomic layer, we used LEIS.[16] Figure 6 shows

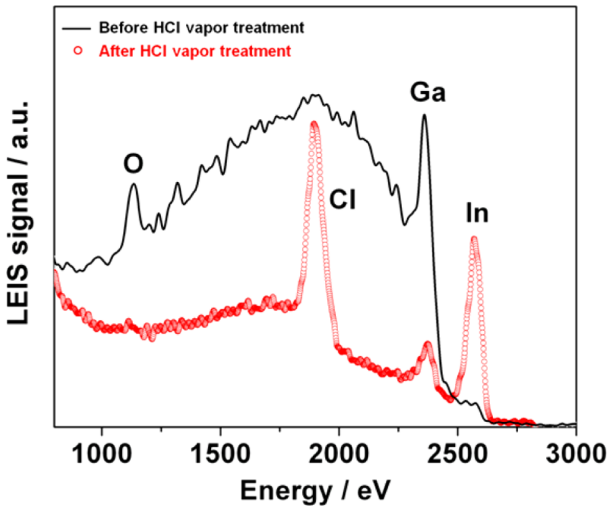


**Figure 6.** LEIS spectra for a Galinstan droplet before and after HCl vapor treatment.

two LEIS spectra of a naturally oxidized Galinstan droplet before and after the HCl vapor treatment. The solid line shows a representative LEIS spectrum of the oxidized Galinstan droplet before the HCl vapor treatment. Before the treatment, the spectrum displayed the peaks of oxygen (at 1130 eV) and of gallium (2362 eV). A small shoulder at 2575 eV may be either from indium or tin that is present inside the Galinstan droplet, since In and Sn peaks cannot be distinguished in the LEIS measurement performed with $^4He^+$. Based on the XPS spectrum, however, we can infer that the main component of the peak at 2572 eV is indium. After the treatment by HCl vapor, the oxygen peak (1130 eV) completely disappeared, and instead, a new peak of chlorine (1895 eV) appeared. In addition, the ratio among the peak intensities of metal components changed. The intensity of the gallium peak decreased while the intensity of the indium peak increased. Combining the results from XPS and LEIS, we conclude that Galinstan under ambient conditions has a gallium oxide layer ($Ga_2O_3$ and $Ga_2O$). However, the exposure to HCl vapor replaces the gallium oxide at the surface layer with a mixture of gallium chloride ($GaCl_3$) and indium chloride ($InCl_3$) with the dominant component of indium chloride (see Figure 6 for the peak intensities).

Indeed, from a thermodynamic point of view, indium(III) chloride is the most stable among the three possible chlorides that can form on the surface of Galinstan after the HCl vapor treatment, because the standard enthalpy of formation of gallium(III) chloride is higher, and it is even higher for tin(II) chloride (see Table 1 for a full list). Comparison between the formation enthalpies explains the reason why indium(III) chloride becomes the dominant phase on the surface of Galinstan after the treatment. One can expect that other phases such as gallium(III) chloride, which is kinetically favored, can also appear after the treatment, and XPS measurements support this hypothesis. Therefore, based on XPS and LEIS studies, the chemical reaction on the surface of oxidized Galinstan with HCl vapor could be described in Figure 7a.

Figure 7b shows an image of the HCl-vapor-treated Galinstan droplet on a Teflon-coated glass slide with an

**Table 1. Standard Enthalpies of Formation of the Most Dominant Chemical Components Composing the Surface of Oxidized Galinstan and Oxidized Galinstan Reacted with HCl**

| chemical compound | standard enthalpy of formation, $\Delta H_F^\circ$ [kJ/mol] |
|---|---|
| $Ga_2O_3$ | −544.6[a] |
| $In_2O_3$ | −462.9[a] |
| SnO | −280.7 |
| $GaCl_3$ | −524.7 |
| $InCl_3$ | −537.2 |
| $SnCl_2$ | −325.1 |

[a]Referenced to the chemical potential of gallium and indium (from ref 25).

illumination. The image clearly shows numerous micrometer-sized droplets of water forming on the surface of Galinstan, as well as relatively larger water pockets at the droplet/substrate interface. We used LyseBlue pH indicator to confirm that those are, indeed, water droplets.

**Bouncing Experiment.** The measured contact angle and surface tension of the HCl-vapor-treated Galinstan droplet suggest that the liquid metal restored its original properties as a nonwetting Newtonian liquid without viscoelasticity. As a further demonstration, bouncing experiments were carried out for a Galinstan droplet (~10 μL) before and after the HCl vapor treatment. The droplet was dropped from a distance of 3.5 cm above the surface of the Teflon-coated glass. High-speed camera (Photron SA4) was used to capture the movement of the droplet with 1000 frames per second. Figure 8 show series of time-lapse images of a droplet of the naturally oxidized Galinstan and the HCl-vapor-treated Galinstan, respectively.

Figure 8a shows both the viscoelasticity and the wetting characteristics of oxidized Galinstan: the falling droplet at 0 ms shows irregular shape with a long tail, suggesting the liquid metal is highly viscoelastic. After the droplet hit the surface, the oxidized Galinstan droplet spread on the surface and never bounced back. On the other hand, Figure 8b demonstrates that the HCl-vapor-treated Galinstan behaves as a simple, non-wetting liquid metal: the falling droplet maintained an almost-spherical shape. After the droplet hit the surface, the HCl-vapor-treated Galinstan droplet readily bounced off from the surface, without leaving any residue on the substrate. These findings confirm our results of the surface analysis from XPS and LEIS. While a natively oxidized Galinstan droplet is expected to build chemical bonds at the interface due to oxide layer, an HCl-vapor-treated Galinstan droplet is not expected to have any chemical bonds, since two halogens (F/Cl) repulse each other, because of their similar dipole moments.

**Reoxidation Experiment.** In order to investigate how stable the transformed surface is in a standard atmosphere, we exposed an HCl-vapor-treated Galinstan droplet to an air environment (at room temperature and 1 atm with a relative humidity (RH) of 30%), and measured the change of its physical and chemical characteristics. First, we measured the static contact angles of an HCl-vapor-treated Galinstan droplet on the Teflon-coated glass every 5 min for 4 h right after the HCl vapor treatment (Figure 9a). The contact angle does not drastically change for the first 20 min, and then gradually decreases to saturate at ~148° after 50 min. The final contact angle (~148°) of the reoxidized droplet is still much closer to the contact angle of an HCl-vapor-treated droplet (~153°) than that of a natively oxidized Galinstan droplet (~141°).


dx.doi.org/10.1021/am302357t | ACS Appl. Mater. Interfaces 2013, 5, 179−185

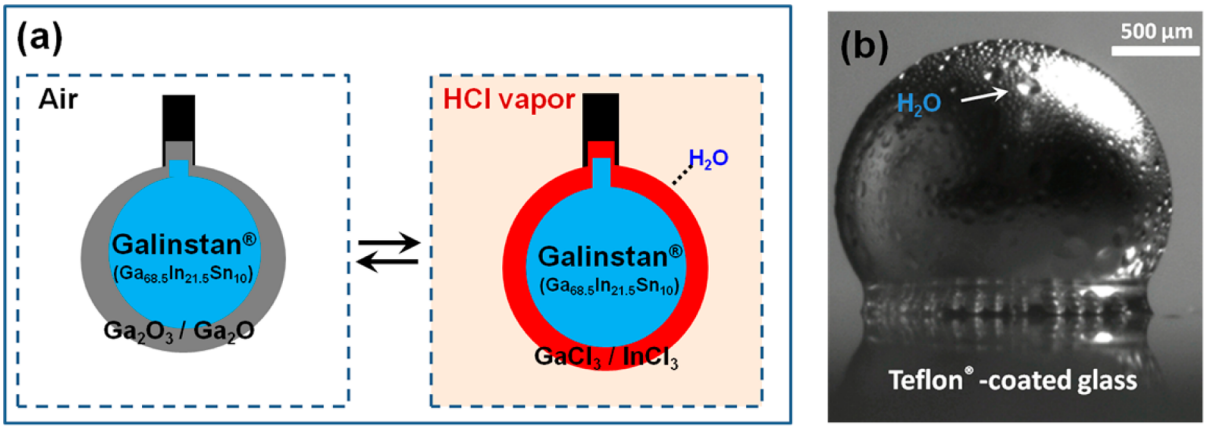


**Figure 7.** (a) Schematic diagram of chemical reaction with HCl vapor. The phase of oxides ($Ga_2O_3$/$Ga_2O$), chlorides ($GaCl_3$/$InCl_3$), and water is solid, aqueous, and liquid, respectively. (b) Optical image of the surface-modified Galinstan droplet on a Teflon-coated glass with an illumination.

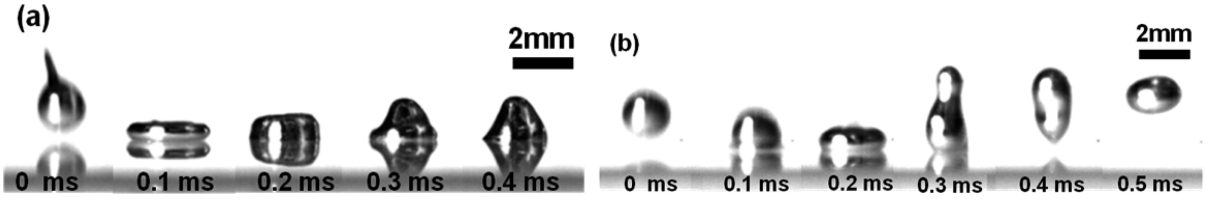


**Figure 8.** Photograph of a series of time-lapse images of (a) a natively oxidized Galinstan droplet and (b) an HCl-vapor-treated Galinstan droplet falling from a distance of 3.5 cm above the surface of Teflon-coated glass.

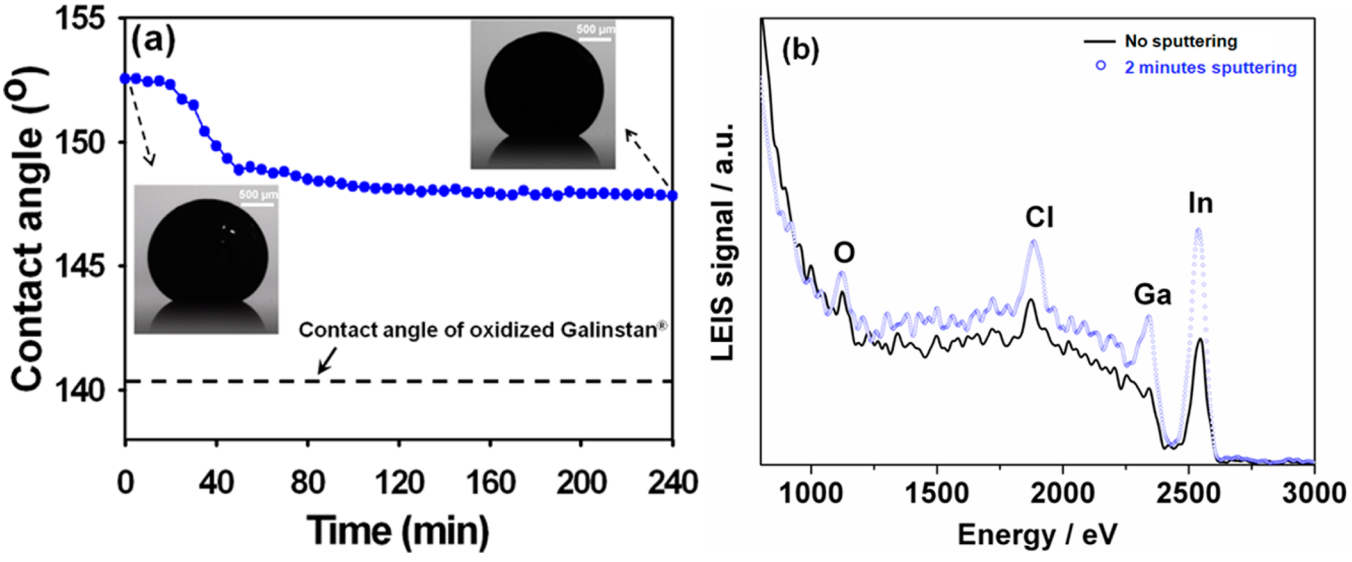


**Figure 9.** (a) Contact angle change of an HCl-vapor-treated Galinstan droplet, plotted as a function of exposure time in the atmosphere. The inset images of the droplet right after the HCl vapor treatment and after the 4 h of reoxidation show that there is no significant difference in contact angles, except a slight change in brightness. (b) LEIS spectra for an HCl-vapor--treated Galinstan droplet after 30 days reoxidation in an air environment.

Therefore, we believe that reoxidation of the surface does happen, but only to a minor degree after 4 h in a standard atmosphere.

In order to investigate the change of surface chemistry, we also exposed an HCl-treated droplet to an air environment for 30 days and analyzed it using LEIS (Figure 9b). The overall intensity of the first measurement (black solid line) is low, because of organic compounds adsorbed on the surface. However, the oxygen peak is visible, which indicates reoxidation has happened. In addition, the intensities of the In and Cl peaks are higher, implying that $InCl_3$ is dominant on the outermost surface, even after 30 days of reoxidation. After a 2 min of sputtering with the 3.0 keV $^4He^+$ beam, clearly the intensity of the Ga peak increased, as well as that of the In and Cl peaks. We believe that the Ga peak is originated from gallium oxide ($Ga_2O_3$, $Ga_2O$) and $GaCl_3$, based on previous XPS and LEIS spectra. The intensity of the Cl peak is higher than the O peak, implying that chlorides are more-dominant components for the inner layer of reoxidized droplets. As a result, even after 30 days of reoxidation, we observed that


dx.doi.org/10.1021/am302357t | ACS Appl. Mater. Interfaces 2013, 5, 179−185

chlorides ($GaCl_3$/$InCl_3$) are dominant components at the liquid metal droplet surface.

## CONCLUSION

The oxide layer on the surface of gallium-based liquid metal alloy causes the alloy to exhibit strong viscoelasticity and adherent characteristics. In this paper, we demonstrated that HCl vapor treatment is a simple yet very effective method to remove the oxide layer on the surface of Galinstan and, eventually, to address the issues of viscoelasticity and wetting. Substantial increase in the contact angle and surface tension of Galinstan was observed after the HCl vapor treatment. We used XPS and LEIS techniques and found that the HCl vapor reacted with the gallium oxide ($Ga_2O_3$ and $Ga_2O$) and indium, each of which is on the surface and in the bulk of Galinstan, respectively. The components of the surface layer thus transformed to gallium chloride ($GaCl_3$) and indium chloride ($InCl_3$), none of which caused the viscoelastic, adherent behavior of Galinstan, as was demonstrated by the bouncing movement of the HCl-vapor-treated Galinstan droplet on a Teflon-coated substrate. The modified surface of the HCl-vapor-treated Galinstan droplet slightly reoxidized when it exposed to an air environment for 30 days, but chlorides still remained as dominant chemical components on the surface. We believe that the proposed method to remove oxide skin from the gallium-based liquid metal is simple and has wide applicability; it can be applied to gallium-based metal droplets of any size, ranging from nanoscale[26,27] to macroscale, without leaving any defect. Therefore, we expect that the proposed method may unleash the full potential of the gallium-based alloy as a nontoxic, nonwetting, Newtonian liquid metal.

## AUTHOR INFORMATION

### Corresponding Author

*E-mail: jblee@utdallas.edu.

### Author Contributions

The manuscript was written through contributions of all of the authors. All of the authors have given approval to the final version of the manuscript.

### Notes

The authors declare no competing financial interest.

## ACKNOWLEDGMENTS

This work was supported in part by the World Class University (WCU) project (No. R32-2009-000-20087-0) funded by the Korean government. The authors would like to acknowledge the DFG and ION-TOF, Jean-Francois Veyan, and the UT Dallas Clean Room staff for their support on this work.

## REFERENCES

(1) Galinstan fluid, Materials Safety Data Sheet (MSDS) No. 93/112/EC [Online]; Geratherm Medical AG: Geschwenda, Germany, March 18, 2004. http://www.rgmd.com/msds/msds.pdf (accessed Nov. 15, 2012).
(2) Dickey, M. D.; Chiechi, R. C.; Larsen, R. J.; Weiss, E. A.; Weitz, D. A.; Whitesides, G. M. *Adv. Funct. Mater.* **2008**, *18*, 1097−1104.
(3) Ma, K.-Q.; Liu, J. *J. Phys. D: Appl. Phys.* **2007**, *40*, 4722−4729.
(4) Kim, H.-J.; Son, C.; Ziaie, B. *Appl. Phys. Lett.* **2008**, *92*, 011904-1−011904-3.
(5) Knoblauch, M.; Hibberd, J. M.; Gray, J. C.; van Bel, A. J. E. *Nat. Biotechnol.* **1999**, *17*, 906−909.
(6) Sen, P.; Chang-Jin, K. *IEEE Trans. Ind. Electron.* **2009**, *56*, 1314−1330.
(7) Irshad, W.; Peroulis, D. *Proceedings of PowerMEMS*, Washington DC, USA, Dec. 1−4, 2009; pp 127−129.
(8) Kubo, M.; Li, X.; Kim, C.; Hashimoto, M.; Wiley, B. J.; Ham, D.; Whitesides, G. M. *Adv. Mater.* **2010**, *22*, 2749−2752.
(9) Meng, L.; Bin, Y.; Behdad, N. *IEEE Microwave Wireless Compon. Lett.* **2010**, *20*, 423−425.
(10) Scharmann, F.; Cherkashinin, G.; Breternitz, V.; Knedlik, C.; Hartung, G.; Weber, T.; Schaefer, J. A. *Surf. Interface Anal.* **2004**, *36*, 981−985.
(11) Tingyi, L.; Sen, P.; Chang-Jin, K. *J. Microelectromech. Syst.* **2012**, *21*, 443−450.
(12) Zrnic, D.; Swatik, D. S. *J. Less-Common Met.* **1969**, *18*, 67−68.
(13) Garrett, A. B.; Lemley, J. *J. Am. Chem. Soc.* **1942**, *64*, 2380−2383.
(14) Lin, S.-Y.; Chen, L.-J.; Xyu, J.-W.; Wang, W.-J. *Langmuir* **1995**, *11*, 4159−4166.
(15) Stauffer, C. E. *J. Phys. Chem.* **1965**, *69*, 1933−1938.
(16) Brongersma, H. H.; Draxler, M.; de Ridder, M.; Bauer, P. *Surf. Sci. Rep.* **2007**, *62*, 63−109.
(17) Quéré, D. *Phys. A* **2002**, *313*, 32−46.
(18) Van Oss, C. J.; Giese, R. F. *Clays Clay Miner.* **1995**, *43*, 474−477.
(19) Cheng, X.; Caironi, M.; Noh, Y.-Y.; Wang, J.; Newman, C.; Yan, H.; Facchetti, A.; Sirringhaus, H. *Chem. Mater.* **2010**, *22*, 1559−1566.
(20) Ray, S. K.; Maiti, C. K.; Lahiri, S. K.; Chakrabarti, N. B. *J. Vac. Sci. Technol., B: Microelectron. Nanometer Struct.* **1992**, *10*, 1139−1150.
(21) Song, Y. P.; Zhang, H. Z.; Lin, C.; Zhu, Y. W.; Li, G. H.; Yang, F. H.; Yu, D. P. *Phys. Rev. B* **2004**, *69*, 075304.
(22) Surdu-Bob, C. C.; Saied, S. O.; Sullivan, J. L. *Appl. Surf. Sci.* **2001**, *183*, 126−136.
(23) Elkashef, N.; Srinivasa, R. S.; Major, S.; Sabharwal, S. C.; Muthe, K. P. *Thin Solid Films* **1998**, *333*, 9−12.
(24) Freeland, B. H.; Habeeb, J. J.; Tuck, D. G. *Can. J. Chem.* **1977**, *55*, 1527−1532.
(25) *CRC Handbook of Chemistry and Physics*, 92nd ed.; CRC Press: Boca Raton, FL, 2012.
(26) Wu, J.; Wang, Z. M.; Li, A. Z.; Benamara, M.; Salamo, G. J. *ACS Appl. Mater. Interfaces* **2011**, *3*, 1817−1820.
(27) Wu, J.; Wang, Z. M.; Dorogan, V. G.; Li, S.; Zhou, Z.; Li, H.; Lee, J.; Kim, E. S.; Mazur, Y. I.; Salamo, G. J. *Appl. Phys. Lett.* **2012**, *101*, 043904-1−043904-4.